Supplemental Figure 1

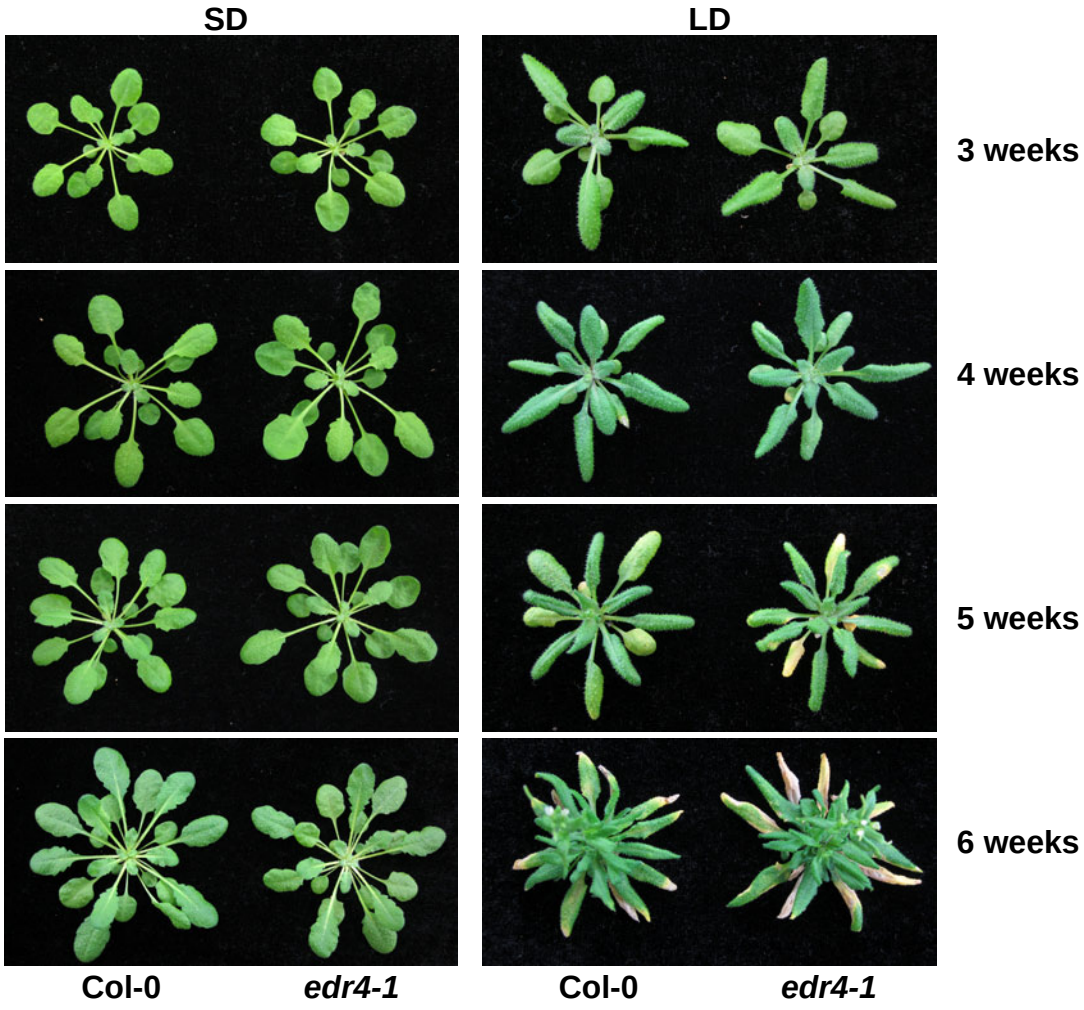

Supplemental Figure 1. The growth phenotype of *edr4-1* mutants under short and long day conditions

The wild type and *edr4-1* plants were grown under short day (SD) or long day (LD) conditions. The photographs were taken at 3, 4, 5, and 6 weeks after germination.

Supplemental Figure 2

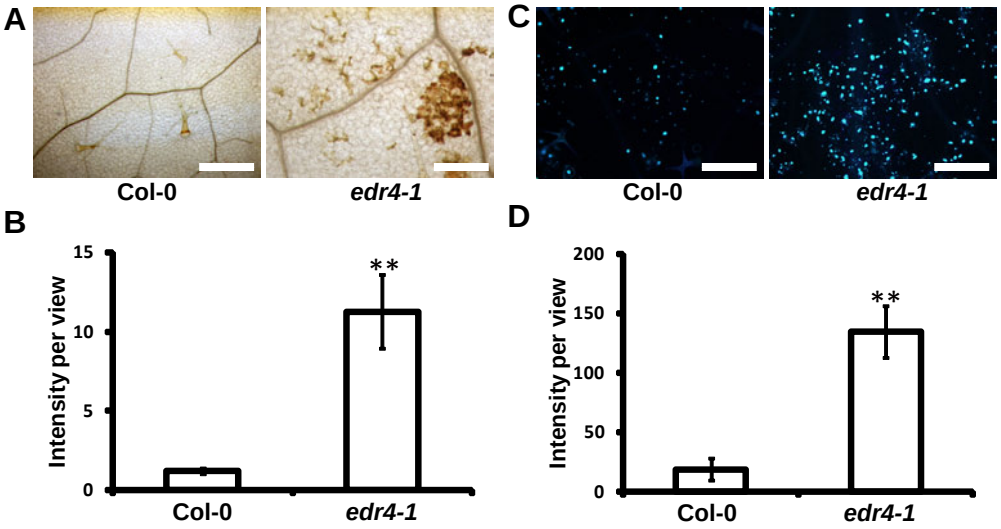

Supplemental Figure 2. Quantification of H_2O_2 and callose accumulation in *edr4-1* after *G. cichoracearum* infection

(A) DAB (diaminobenzidine) staining of four-week-old wild type and *edr4-1* mutants at 2 DAI with *G. cichoracearum*. Bars=0.5 mm.

(B) Quantitative analysis of H_2O_2 production in four-week-old wild type and *edr4-1* mutants at 2 DAI.

(C) Aniline blue staining for callose deposition in four-week-old wild type and *edr4-1* mutants at 2 DAI with *G. cichoracearum*. Bars=1 mm.

(D) Quantitative analysis of callose accumulation in four-week-old wild type and *edr4-1* mutants at 2 DAI.

In (B) and (D), the bars represent the mean and standard deviation of intensity per view from six leaves of three plants for each genotype. The experiment was repeated three times with similar results. Asterisks indicate a significant difference from the wild type ($P < 0.01$; Student's t-test).

Supplemental Figure 3

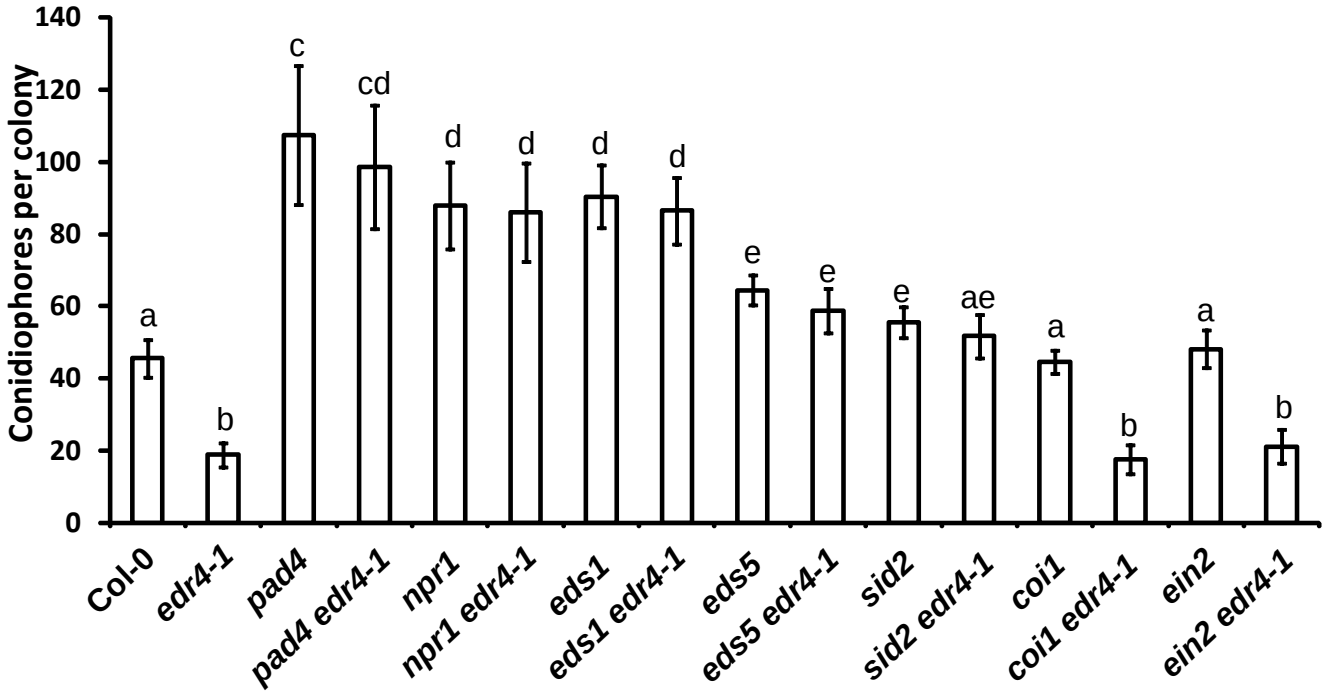

Supplemental Figure 3. Quantitative analysis of conidiophore formation on inoculated leaves of wild type, *edr4-1*, and different double mutant plants with *G. cichoracearum* at 6 DAI. The bars represent mean and standard deviation (n=20). The experiment was repeated three times with similar results. Statistically significant differences among the samples are labeled with different letters (*P<0.01*, one-way ANOVA).

Supplemental Figure 4

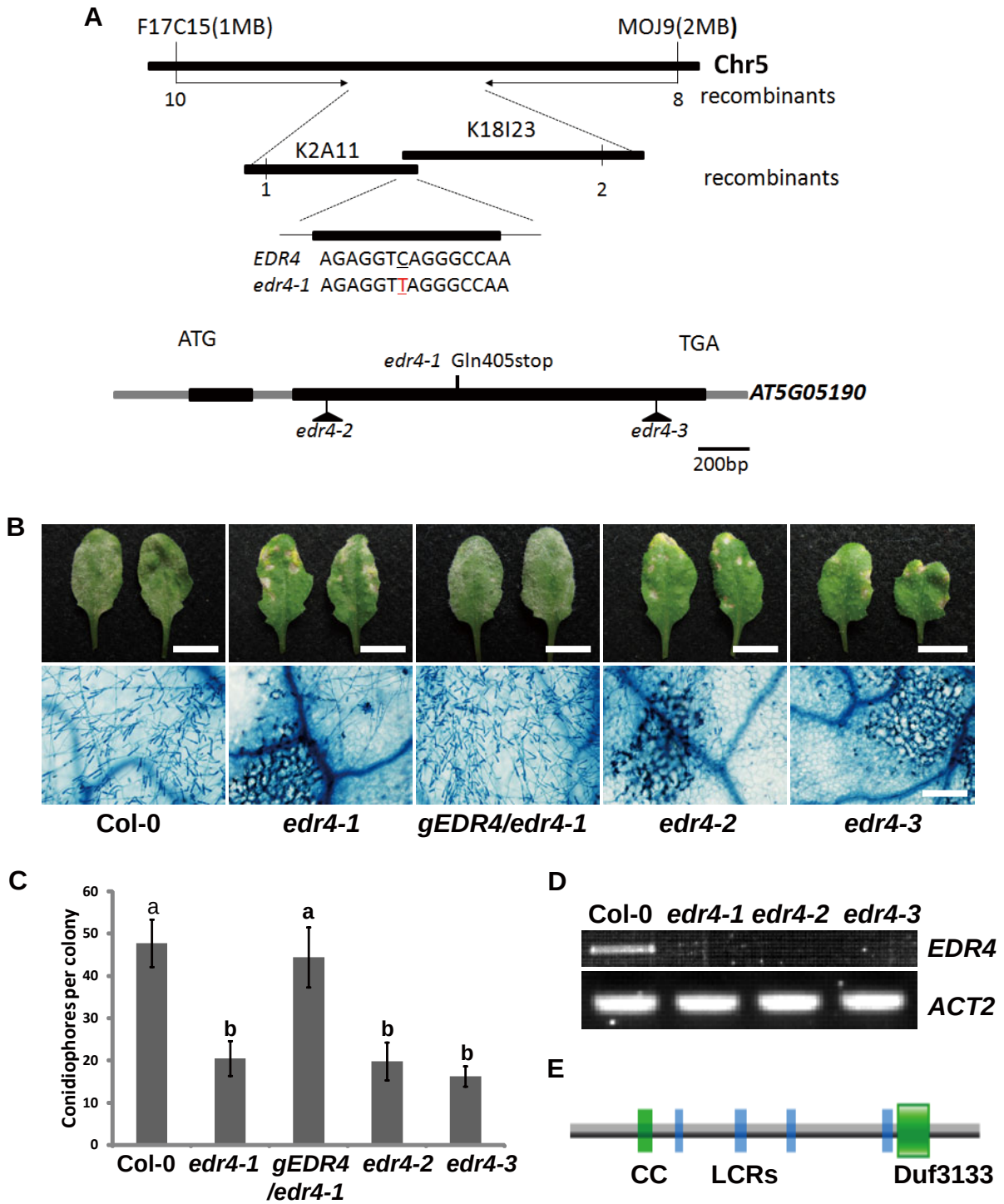

Supplemental Figure 4. Identification and complementation of the *edr4-1* mutation

(A) The *edr4-1* mutation was identified by map-based cloning. The BAC clones and number of recombinants identified are indicated. The *edr4-1* point mutation is labeled in red. The exons are indicated by black-shaded boxes; introns and UTRs are indicated by grey-shaded boxes. Position of the *edr4-1* mutation and the T-DNA insertion sites in the *edr4-2* and *edr4-3* lines are indicated.

(B) Complementation of the *edr4-1* mutation by a genomic clone of *EDR4*. Upper panel, photograph of representative leaves removed from four-week-old plants at 8 DAI with *G. cichoracearum*. Bars=0.5 cm. Lower Panel: Trypan Blue staining of the infected leaves, Bar=100 µm.

(C) Quantitative analysis of conidiophore formation on plants at 6 DAI. The bars represent mean and standard deviation (n=20). The experiment was repeated three times with similar results. Statistically significant differences among the samples are labeled with different letters (P<0.01, one-way ANOVA).

(D) The expression of *EDR4* in four-week-old plants by RT-PCR, with expression of *ACT2* as the internal control.

(E) Protein structure of EDR4. The coiled-coil domain is indicated with green stripes, the Duf3133 domain by a green box, and low-complexity regions with blue stripes.

Supplemental Figure 5

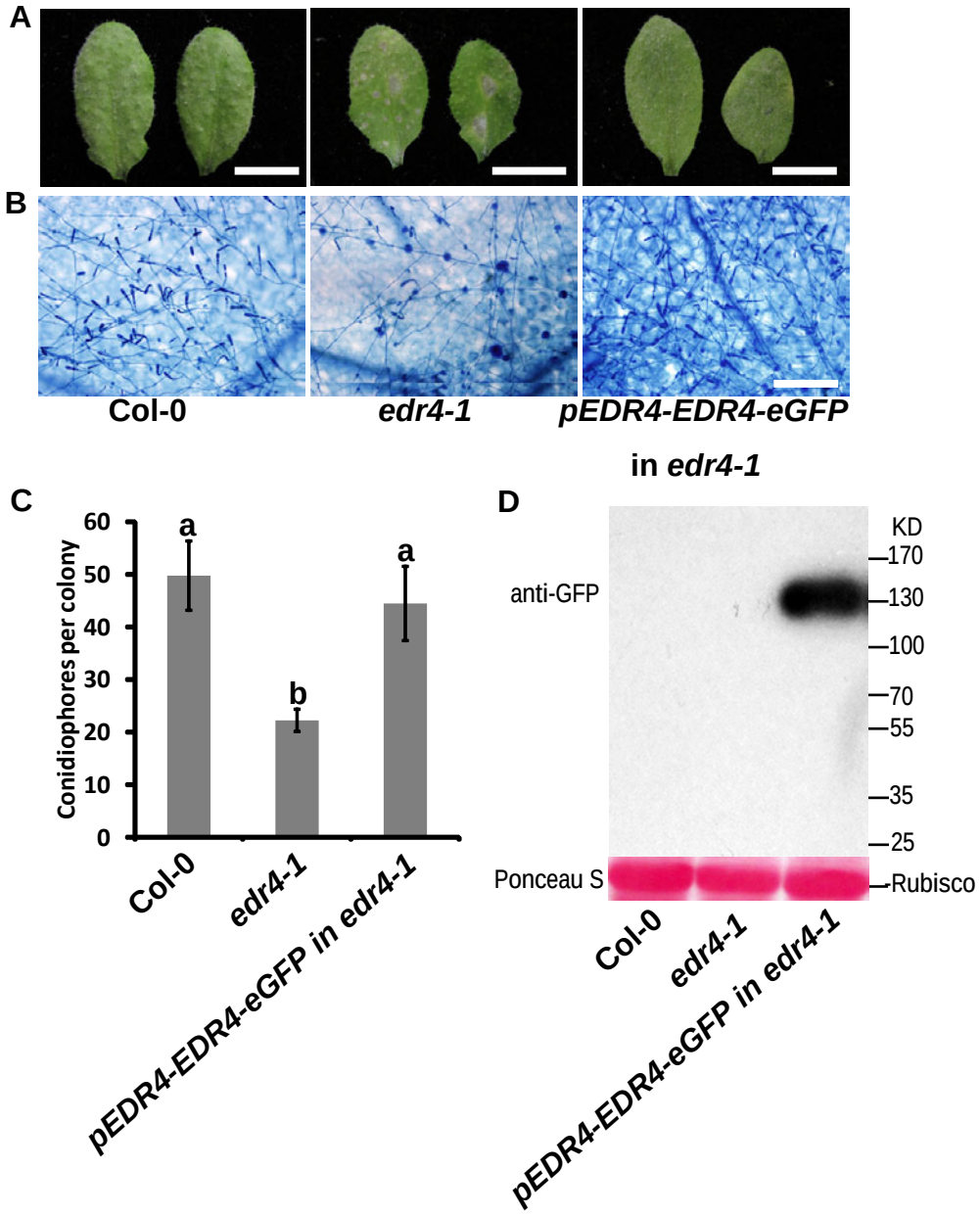

Supplemental Figure 5. EDR4-GFP fusion protein complemented the *edr4-1* powdery mildew resistance phenotype

(A) Representative leaves removed from infected plants at 8 DAI. Bars=0.5 cm.

(B) Trypan Blue staining of (A), to visualize fungal structure and plant cell death. Bar=100 µm.

(C) Quantitative analysis of conidiophore formation at 6 DAI. The bars represent mean and standard deviation (n=20). The experiment was repeated three times with similar results. Statistically significant differences among the samples are indicated with different letters (P<0.01, one-way ANOVA).

(D) EDR4-GFP protein was expressed as full-length protein in 4-week-old *pEDR4-EDR4-eGFP edr4-1* transgenic plants. Immunoblotting was performed using anti-GFP antibody. Ponceau S staining of Rubisco is shown as a loading control.

Supplemental Figure 6

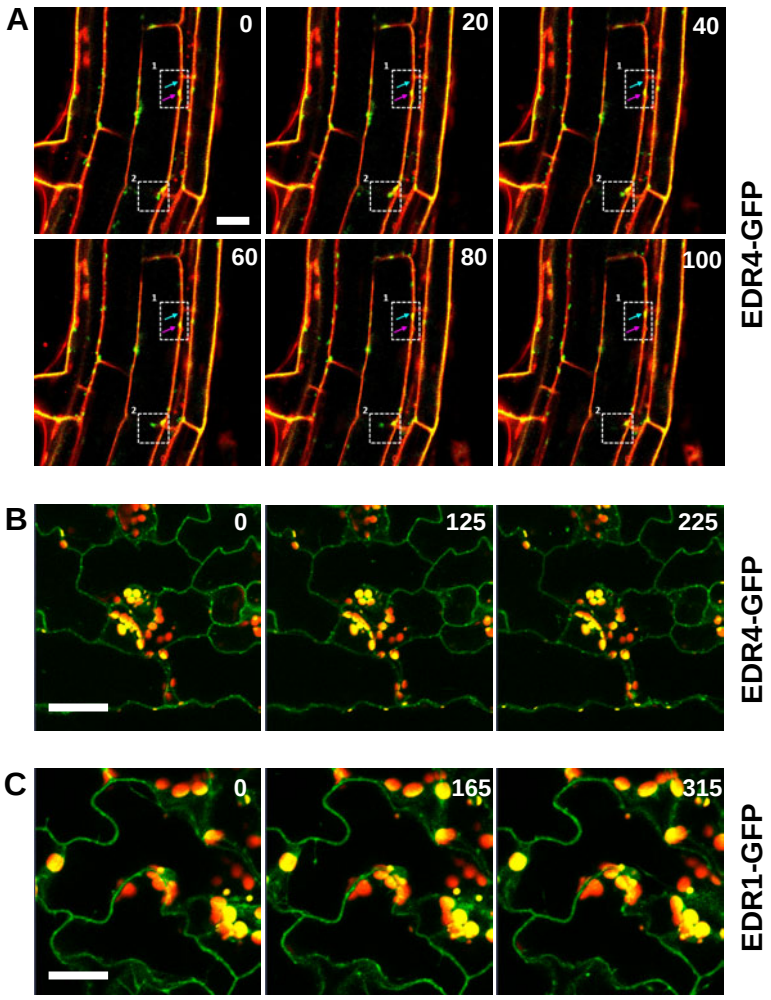

Supplemental Figure 6. Selected frames of Supplemental Movies 1, 2, and 3. The starting time is set as 0, and representative individual images were selected at the indicated times, in seconds, shown at the top left.

(A) Representative time-lapse images of EDR4-GFP intracellular trafficking in the cell elongation zone of the root of a five-day-old transgenic seedling. Images were taken with a confocal microscope. The dotted box labeled “1” shows EDR4 that colocalized with FM4-64; the box labeled “2” shows some EDR4 protein that did not colocalize with FM4-64. The arrows with different colors show the movement of EDR4 and FM4-64. Bar=20 µm.

(B) -(C) First, middle, and last frames of EDR4-GFP (B) or EDR1-GFP (C) intracellular trafficking in a leaf epidermal cells from four-week-old transgenic plants. Red signal shows chloroplasts. Bar=50 µm (B) or 25 µm (C).

Supplemental Figure 7

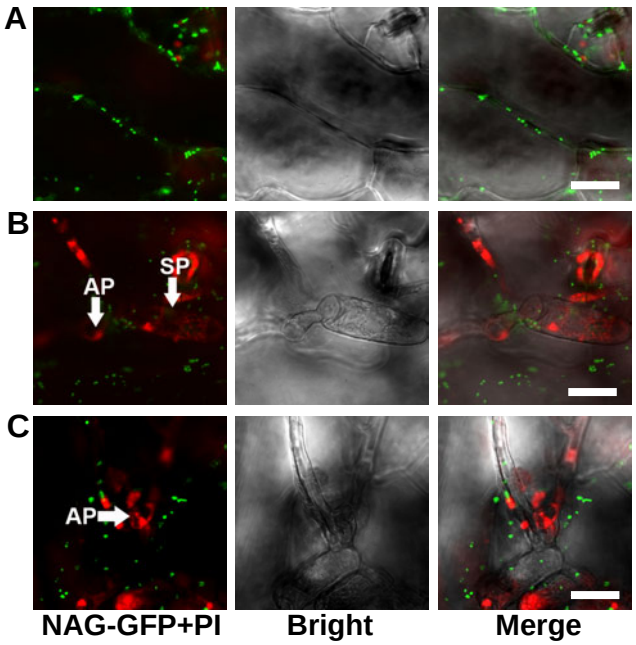

Supplemental Figure 7. NAG-GFP proteins did not accumulate at the penetration site upon *G. cichoracearum* infection.

(A) NAG-GFP localizes in *cis*-Golgi in epidermal cells of uninfected leaves. Bar=50 μm.

(B) and (C) No accumulation of NAG-GFP around the penetration peg at 24 HAI with *G. cichoracearum*. Bars=50 μm. Leaves were stained with propidium iodide (red) to visualize the fungal structures.

AP, appressoria; SP, spores.

Supplemental Figure 8

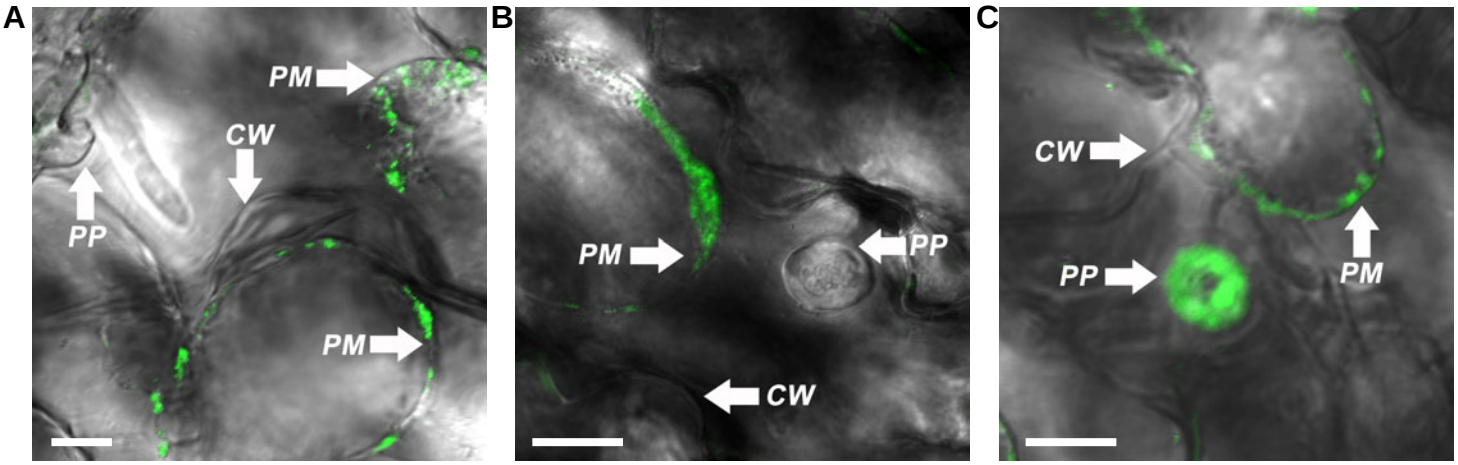

EDR4-GFP **EDR1-GFP** **PEN1-GFP**

Supplemental Figure 8. EDR4 and EDR1 localize to the plasma membrane, not papillae.

Four-week-old plants were infected with *G. cichoracearum* and are shown at 24 HAI. Plasmolysis of epidermal cells expressing EDR4-GFP (A), EDR1-GFP (B) and PEN1-GFP (C), as observed by confocal microscopy. Bars=8 µm. EDR4-GFP and EDR1-GFP fluorescence was detected in the plasma membrane, not in the papillae surrounding the fungal penetration peg. PM: plasma membrane, PP, penetration peg, CW: cell wall.

Supplemental Figure 9

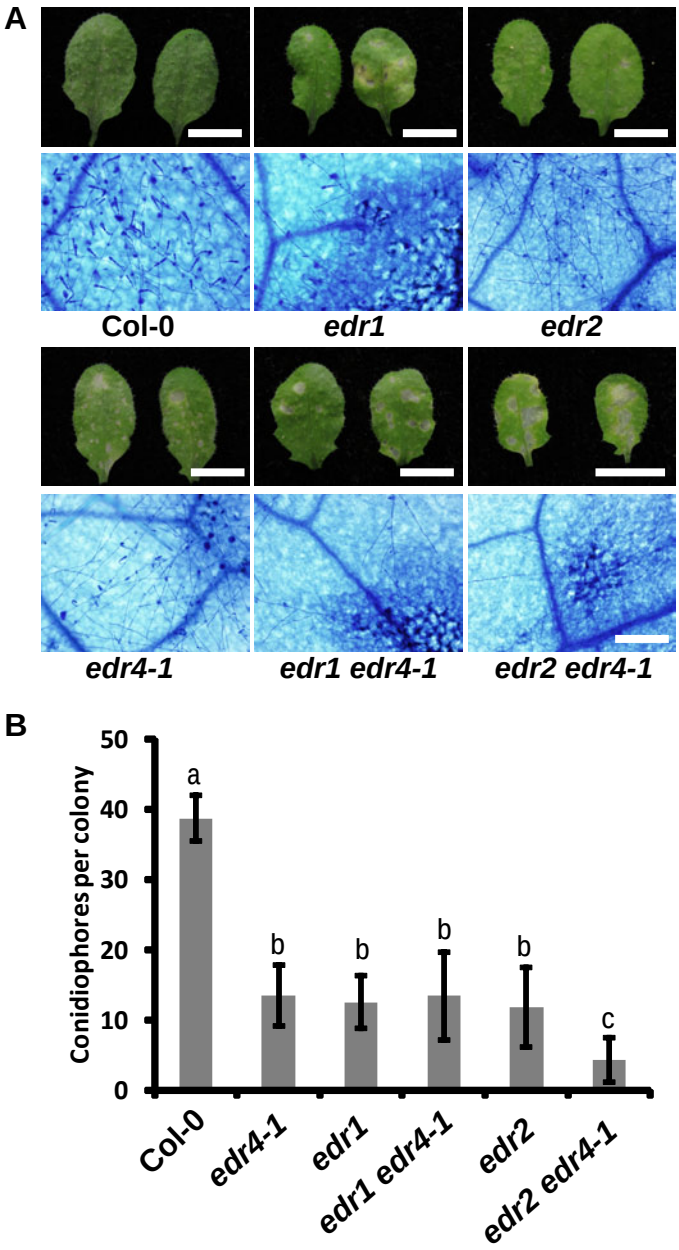

Supplemental Figure 9. The *edr2* mutation enhances the *edr4*-mediated powdery mildew resistance phenotype

(A) Photograph and Trypan Blue staining of representative leaves removed from four-week-old plants at 8 DAI with *G. cichoracearum*. Upper panel: Bars=0.5 cm. Lower panel: Bar=100 µm.

(B) Quantitative analysis of conidiophore formation on infected plants at 6 DAI. The bars represent mean and standard deviation (n=20). The experiment was repeated three times with similar results. Statistically significant differences among the samples are labeled with different letters (P<0.01, one-way ANOVA).

Supplemental Figure 10

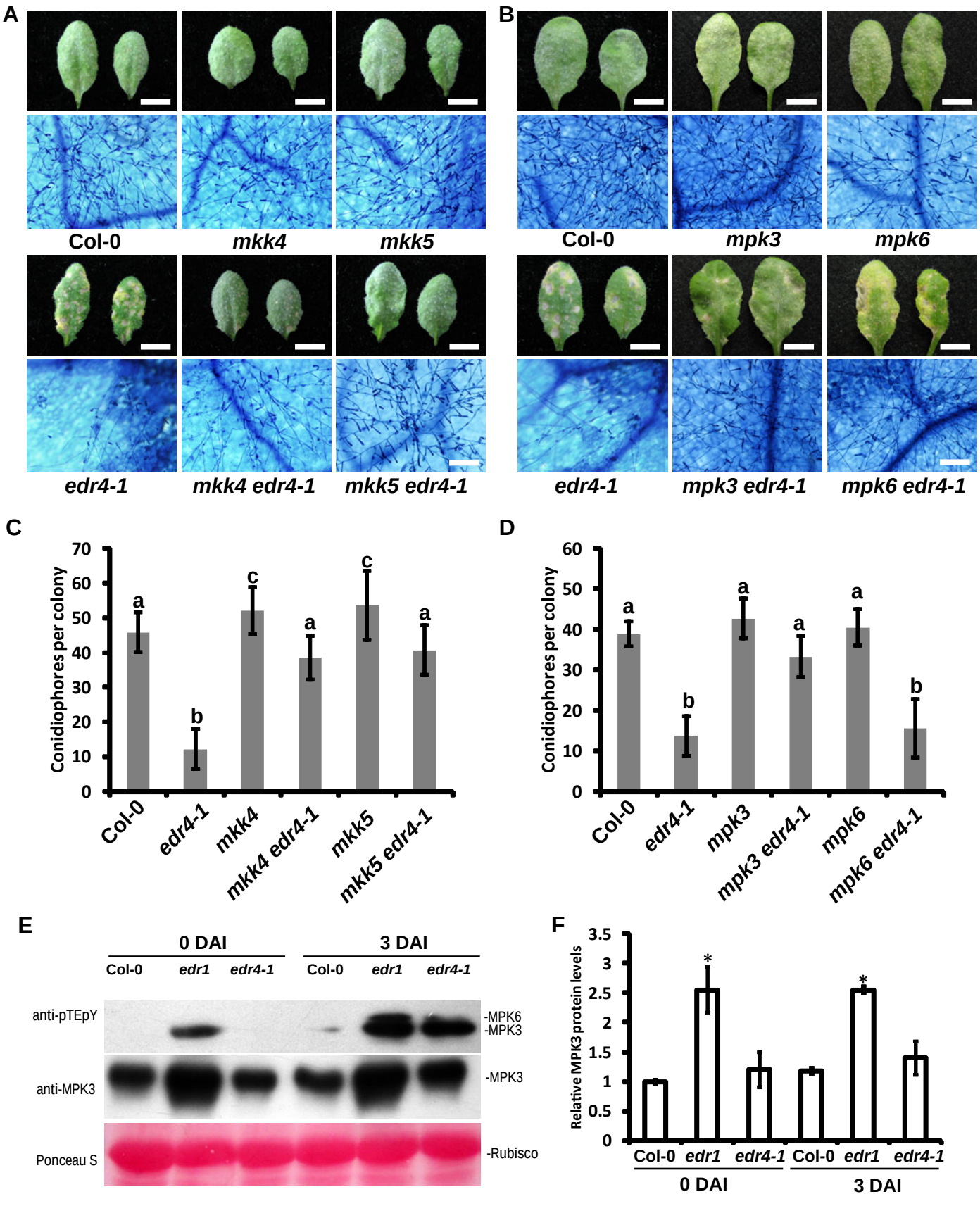

Supplemental Figure 10. *edr4*-mediated resistance requires the MAPK pathway

(A) The *mkk4* and *mkk5* mutations suppress *edr4-1*-mediated resistance. Upper panel: Photograph of representative leaves from four-week-old wild type, *edr4-1*, *mkk4*, *mkk4 edr4-1*, *mkk5*, and *mkk5 edr4-1* plants at 8 DAI with *G. cichoracearum*. Bars=0.5 cm. Lower panel: Trypan Blue staining of infected leaves at 8 DAI, Bar=100 µm.

(B) The *mpk3* mutation partially suppresses *edr4-1*-mediated resistance. Photograph and Trypan Blue staining of representative leaves removed from four-week-old plants inoculated with *G. cichoracearum* at 8 DAI. Upper panel: Bars=0.5 cm; Lower panel: Trypan Blue staining, Bar=100 µm.

(C) Quantitative analysis of conidiophore formation on infected plants shown in (A), at 6 DAI. The bars represent mean and standard deviation (n=35). The experiment was repeated three times with similar results. Statistically significant differences are labeled with different letters (P<0.01, one-way ANOVA).

(D) Quantitative analysis of conidiophore formation on infected plants shown in (B), at 6 DAI. The bars represent mean and standard deviation (n=20). The experiment was repeated three times with similar results. Statistically significant differences are labeled with different letters (P<0.01, one-way ANOVA).

(E) Differential MPK activation in four-week-old wild type, *edr1*, and *edr4-1* plants after powdery mildew infection, as shown by immunoblot analysis using anti-pTEpY antibody. Individual MPKs are identified by molecular mass. The anti-MPK3 antibody shows MPK3 protein levels. Ponceau S staining of Rubisco is shown as a loading control.

(F) Relative MPK3 protein levels in (E) were calculated with uninfected wild type as the internal control, using ImageJ software. The bars represent mean and standard deviation (n=4). The asterisk indicates a significant difference from wild type (P<0.01. Student’s t-test).

Supplemental Figure 11

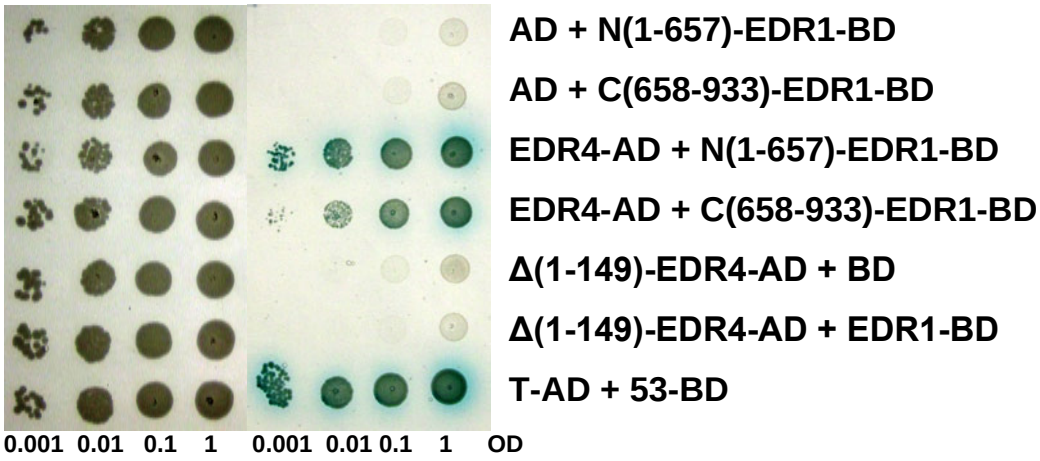

Supplemental Figure 11. EDR4 interacts with N-terminal domain of EDR1 in yeast two-hybrid assays.

Yeast colonies containing the indicated plasmids were serially diluted from OD_{600}=1 and dropped on SD/-Leu/-Trp or on SD/-His/-Leu/-Trp supplemented with 25 mM 3-amino-1,2,4-triazole and 40 μg/mL X-α-Gal. AD: pGADT7, BD: pGBKT7, T-AD + 53-BD was used as a positive control. ΔCC-EDR4 lacks the amino acids 1-149, which includes the coiled-coil domain. N(1-657)-EDR1, the 1-657th amino acids of EDR1; C(658-933), the 658-933th amino acids of EDR1.

Supplemental Figure 12

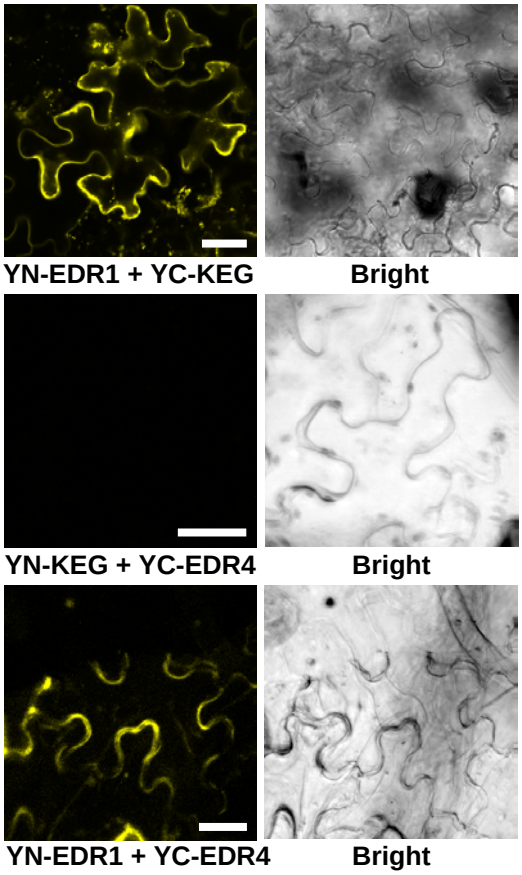

Supplemental Figure 12. EDR4 interacts with EDR1, not KEG, *in vivo*

EDR4 interacted with EDR1 in BiFC assays in *N. benthamiana*. EDR1 was fused to the N-terminal fragment of YFP and EDR4 was fused to the C-terminal fragment of YFP. The combination of YN-EDR1 and YC-KEG was used as the positive control. YFP fluorescence indicates an interaction between the two proteins. Bars=25 µm. These experiments were repeated three times with similar results.

Supplemental Figure 13

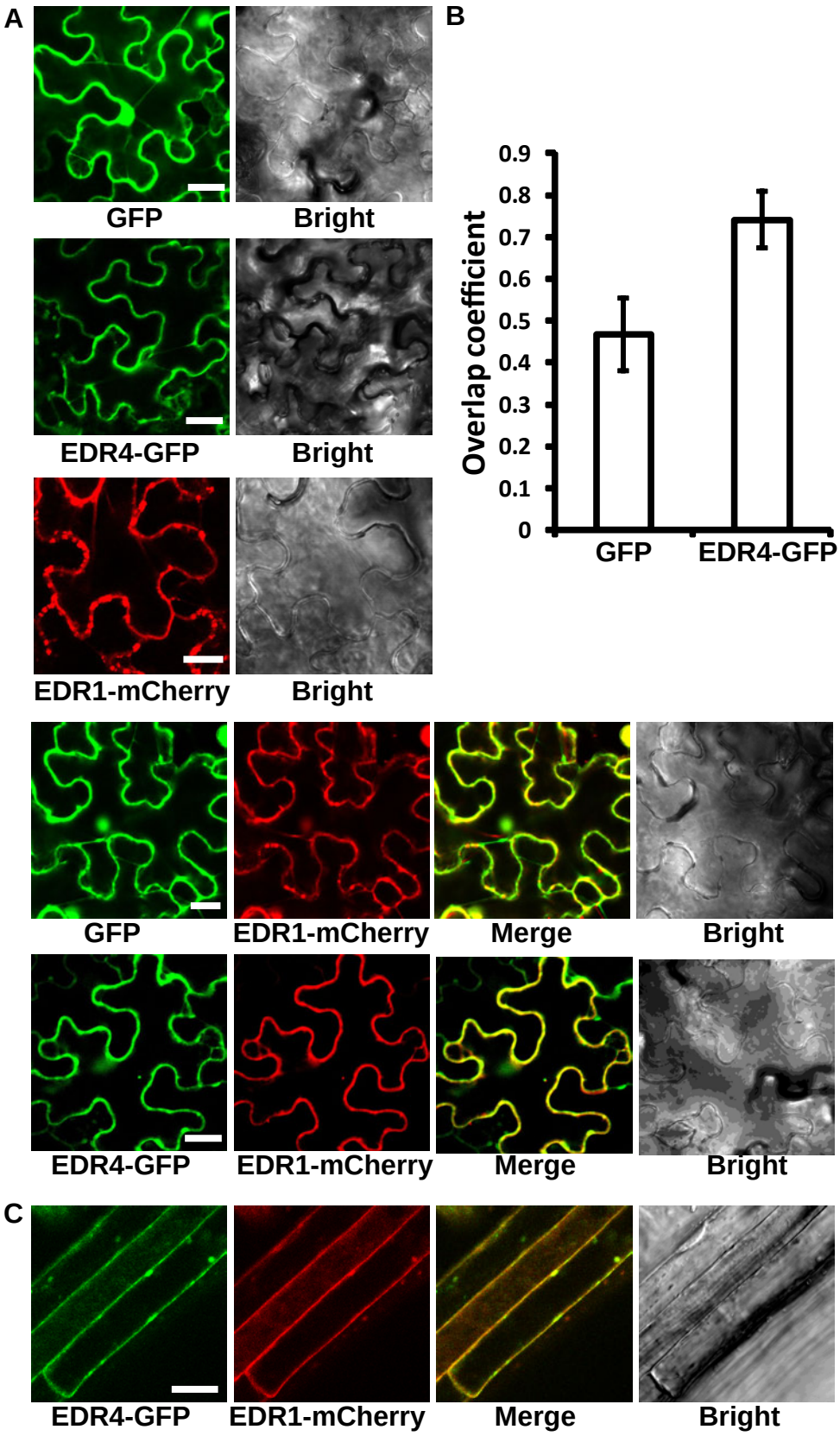

Supplemental Figure 13. EDR4 co-localizes with EDR1.

(A) EDR1-mCherry co-localizes with EDR4-GFP in *N. benthamiana*. GFP, EDR4-GFP, EDR1-mCherry, GFP and EDR1-mCherry, or EDR4-GFP and EDR1-mCherry were transiently expressed respectively in *N. benthamiana*. Chl: chloroplast. Bars=25 µm.

(B) Quantitative analysis of the overlap of EDR1-mCherry with GFP and EDR4-GFP. The bars show Mander's overlap coefficient (Herda et al., 2012) indicating the level of colocalization of EDR1-mCherry with GFP or EDR4-GFP. Two independent experiments with 20 co-transformed cells for each subcellular marker were evaluated.

(C) Co-localization of EDR1-mCherry and EDR4-GFP in elongating root cells of five-day-old *Arabidopsis* plants. Bar=20 µm.

Samples were observed and imaged by confocal microscopy.

Supplemental Figure 14

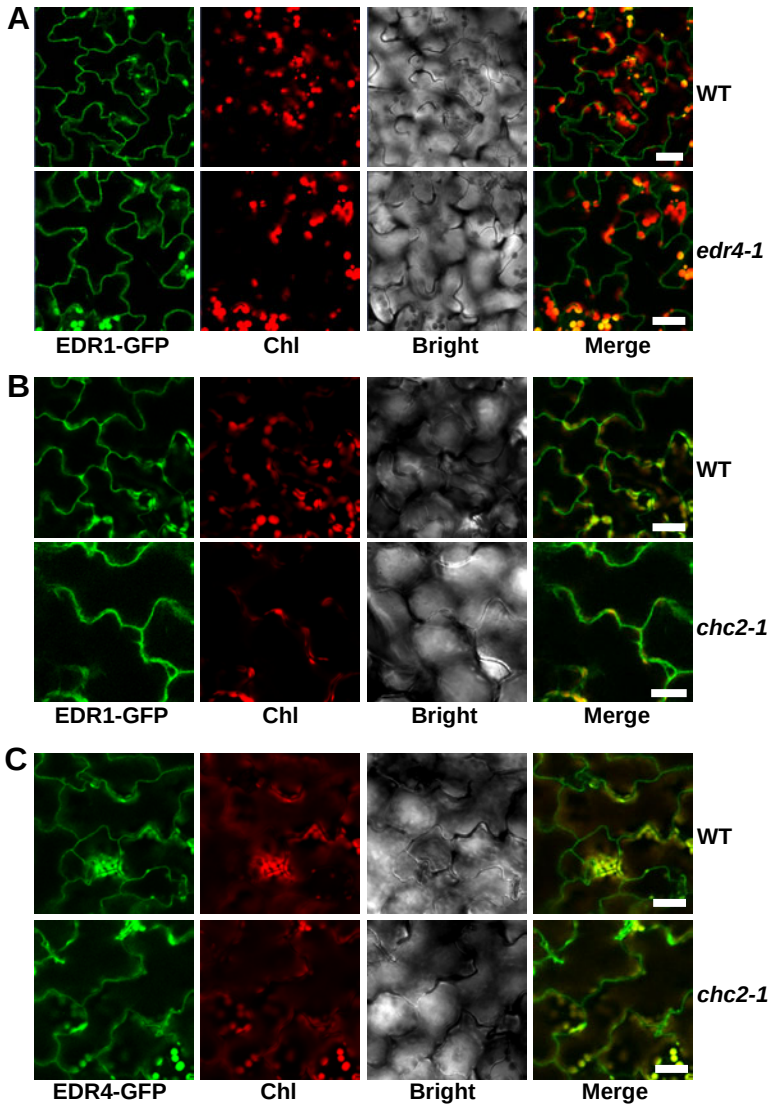

Supplemental Figure 14. The *edr4-1* and *chc2-1* mutations did not affect EDR1-GFP localization in uninfected leaves.

GFP signal was observed from epidermal cells of uninfected four-week-old plants.

(A) Localization of EDR1-GFP in wild type and *edr4-1* plants.

(B) Localization of EDR1-GFP in wild type and *chc2-1* plants

(C) Localization of EDR4-GFP in wild type and *chc2-1* plants.

Chl, chloroplast; Bars=25 μm.

Supplemental Figure 15

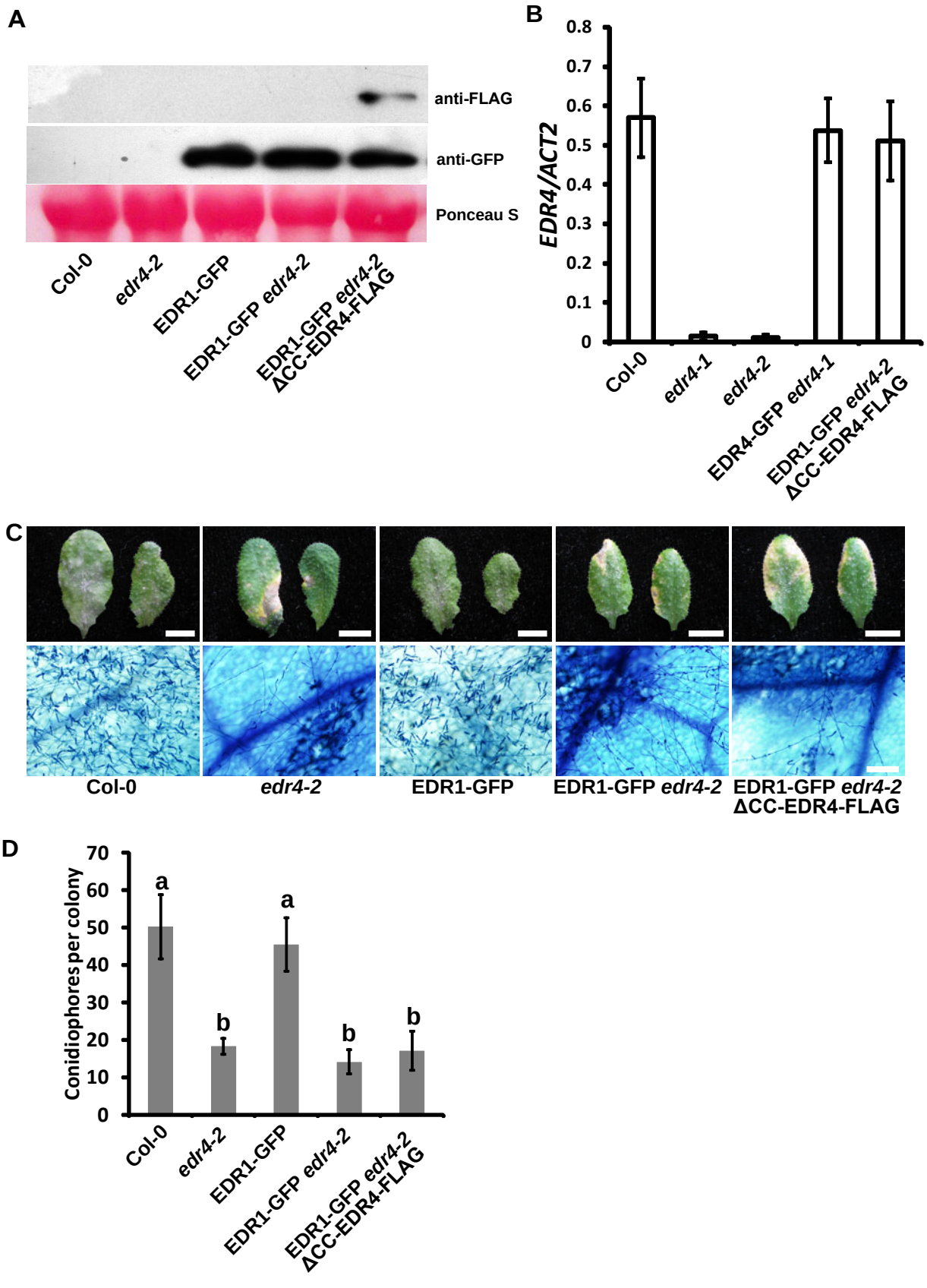

Supplemental Figure 15. The EDR4 coiled-coil domain is required for EDR4 function.

(A) The native promoter-driven ΔCC-EDR4-FLAG (lacks 1-149aa of EDR4) was introduced into *edr4-2* and EDR1-GFP *edr4-2* plants. Accumulation of Δ CC-EDR4 protein and EDR1-GFP was examined by immunoblot analysis using anti-FLAG or anti-GFP antibody, respectively. Ponceau S staining of Rubisco is shown as a loading control.

(B) Real-time PCR to examine *EDR4* expression levels in 14-day-old seedlings of wild type, *edr4-1*, *edr4-2*, EDR4-GFP *edr4-1*, and ΔCC-EDR4-FLAG EDR1-GFP *edr4-2* plants. The experiments were repeated three times with similar results.

(C) Photograph (upper panel) and Trypan Blue staining (lower panel) of representative leaves removed from four-week-old wild type, *edr4-2*, EDR1-GFP, EDR1-GFP *edr4-2* and ΔCC-EDR4-FLAG EDR1-GFP *edr4-2* plants at 8 DAI with *G. cichoracearum*. Upper panel: Bars=0.5 cm. Lower panel: Bar=100 μm.

(D) Quantitative analysis of conidiophore formation on infected plants at 6 DAI. The bars represent mean and standard deviation (n=15). The experiment was repeated three times with similar results. Statistically significant differences among the samples are labeled with different letters (P<0.01, one-way ANOVA).

Supplemental Figure 16

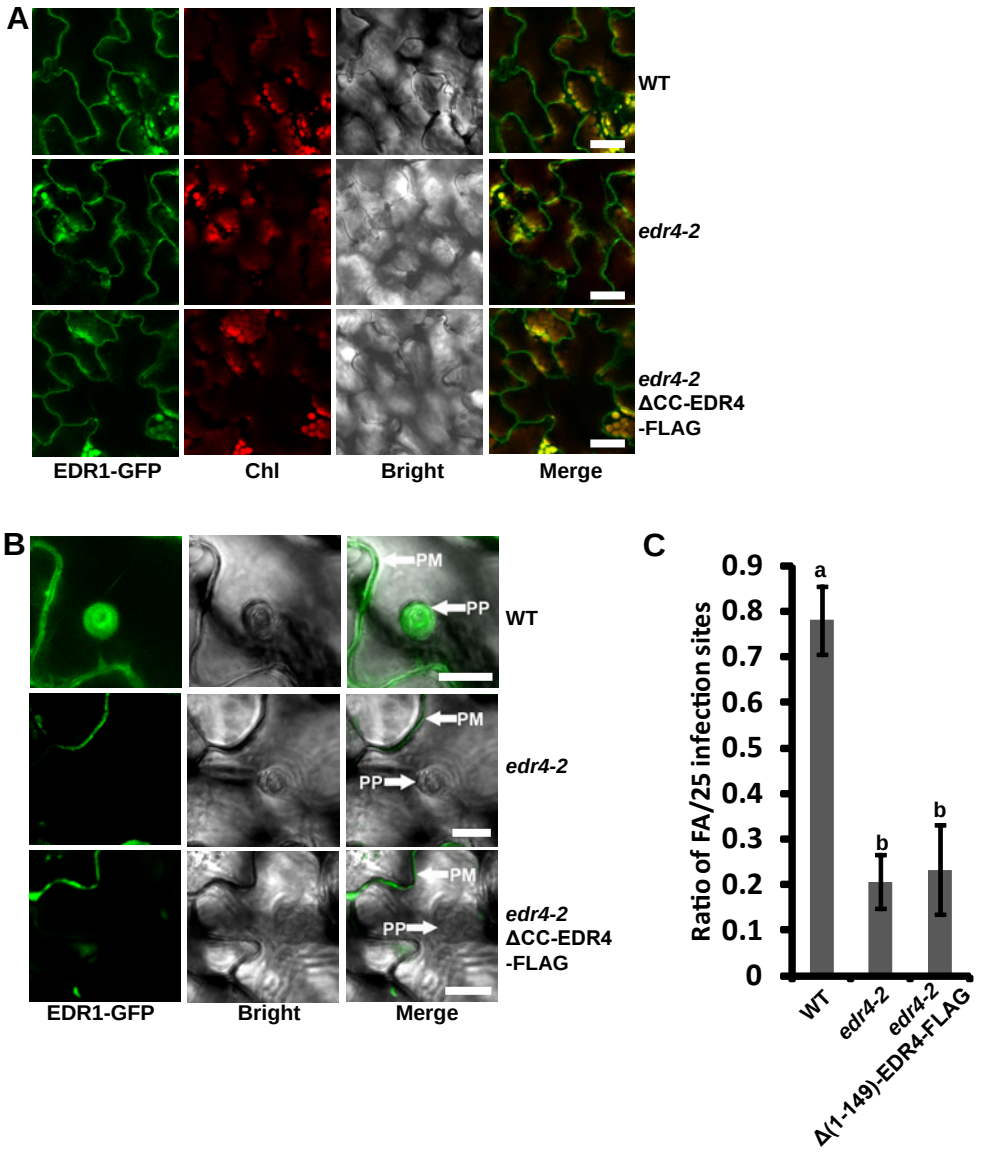

Supplemental Figure 16. EDR1-GFP localization in an EDR4-CC-domain deletion background.

(A) Localization of EDR1-GFP in epidermal cells of uninfected four-week-old wild type, *edr4-2* and *edr4-2* ΔCC-EDR4-FLAG plant leaves. Chl, chloroplast; Bars=35 µm.

(B) Four-week-old plants were infected with *G. cichoracearum* and localization of EDR4-GFP in wild type, *edr4-2* and *edr4-2* ΔCC-EDR4-FLAG plants are shown at 24 HAI. Bars=8 µm. PM: plasma membrane, PP, penetration peg.

(C) Quantitative analysis of EDR1-GFP focal accumulations in wild type, *edr4-2* and *edr4-2* ΔCC-EDR4-FLAG plants. Bars represent mean and standard deviation of values obtained from three biological replicates per genotype. Statistically significant differences among the samples are labeled with different letters (*P*<0.01, one-way ANOVA). The experiments were repeated three times with similar results.

Supplemental Figure 17

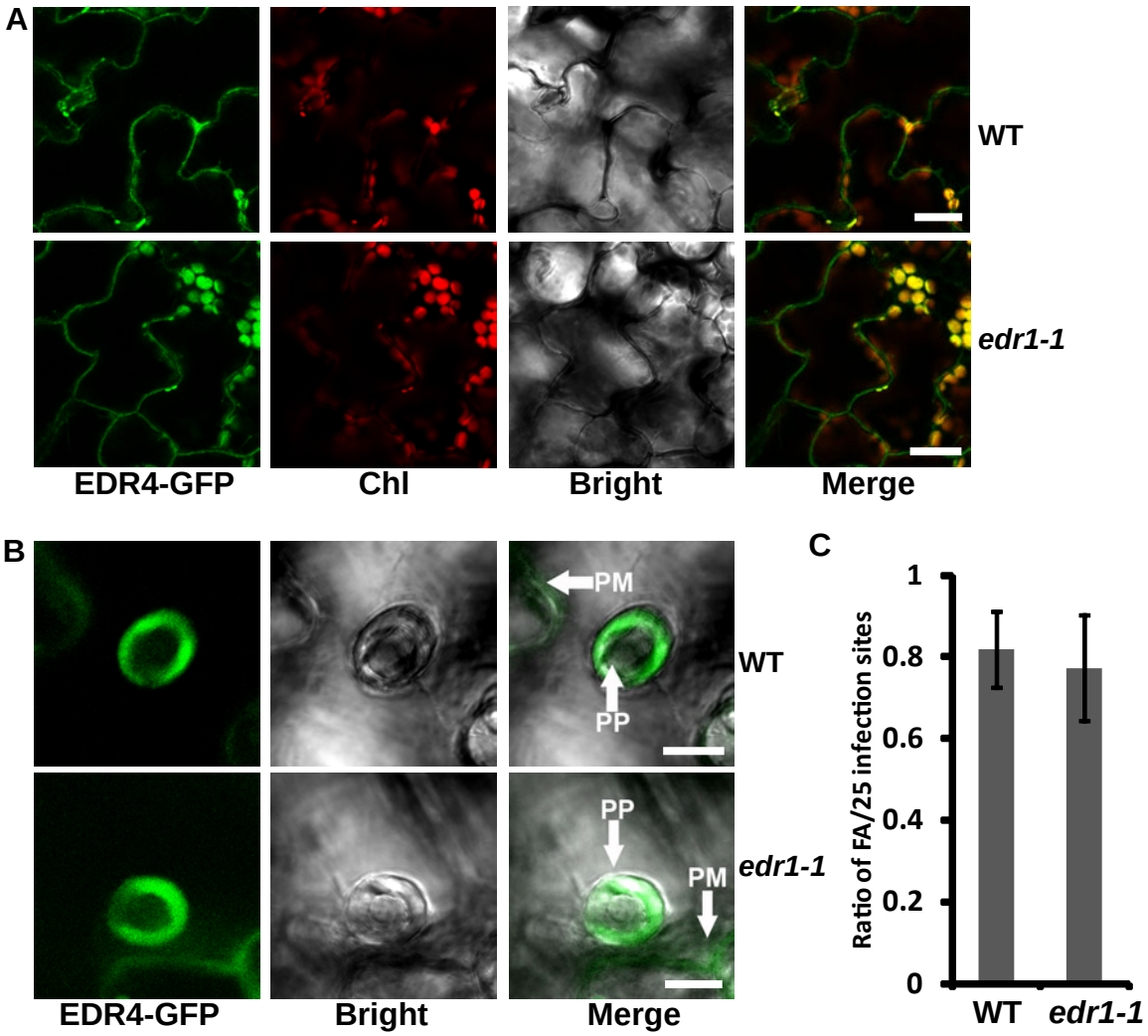

Supplemental Figure 17. The *edr1-1* mutation did not affect EDR4-GFP localization in uninfected and infected leaves.

(A) Localization of EDR4-GFP in uninfected four-week-old wild type and *edr1-1* plants. Chl, chloroplast; Bars=25 µm.

(B) Four-week-old plants were infected with *G. cichoracearum* and localization of EDR4-GFP in wild type and *edr1-1* plants are shown at 24 HAI. Bars=10 µm. PM, plasma membrane; PP, penetration peg

Supplemental Figure 18

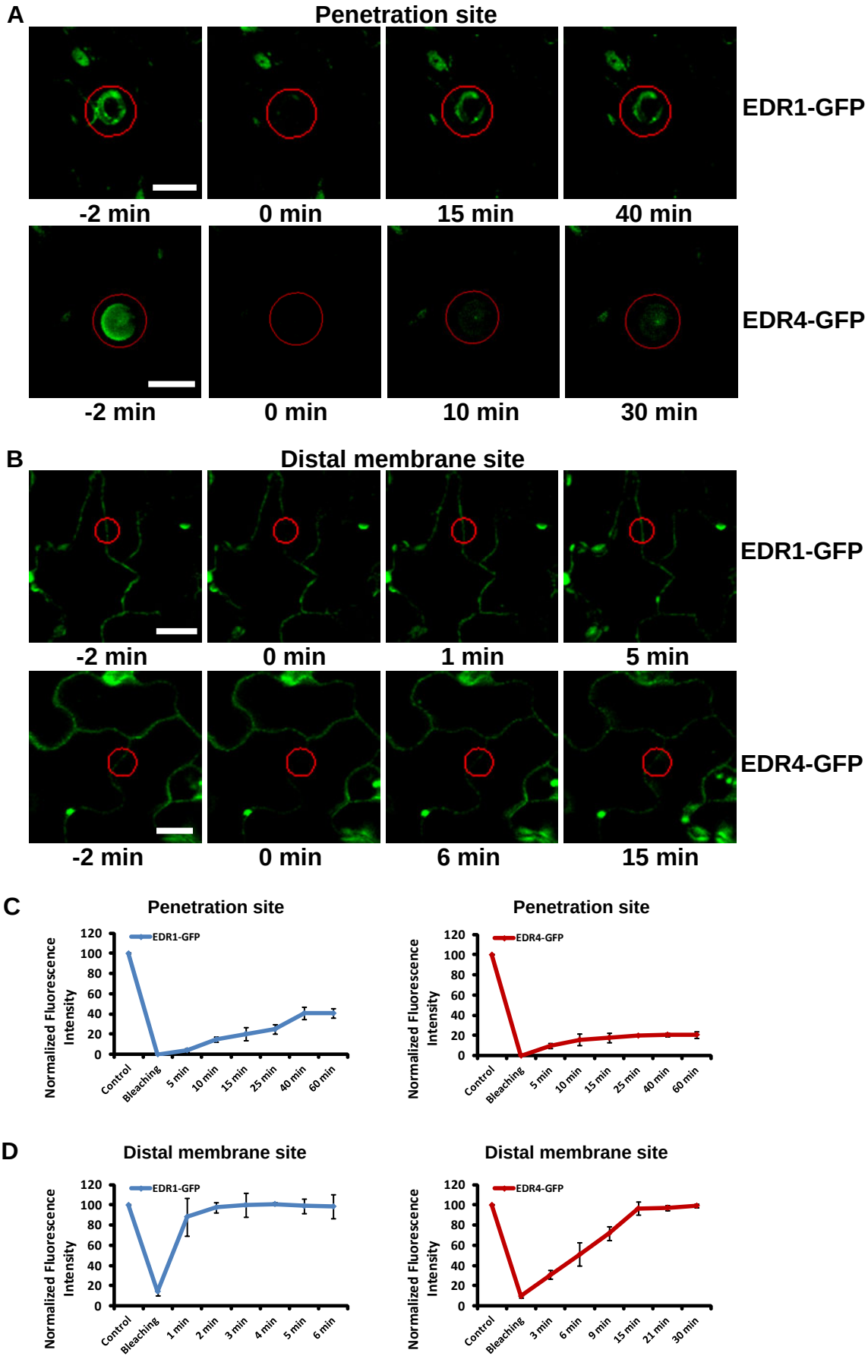

Supplemental Figure 18. FRAP analysis of EDR1-GFP and EDR4-GFP focal accumulation at powdery mildew penetration sites

(A) FRAP analysis of EDR1-GFP and EDR4-GFP was performed at penetration sites of epidermal cells at 24 HAI with *G. cichoracearum*. The images were taken before (-2 min), immediately after (0 min), and at various time points after photobleaching. Bars=20 µm.

(B) FRAP analysis of EDR1-GFP and EDR4-GFP was performed at distal membrane sites of epidermal cells at 24 HAI with *G. cichoracearum*. Bars=20 µm.

(C-D) Quantitative analysis of EDR1-GFP and EDR4-GFP fluorescence intensity at penetration and distal membrane sites at various time points after photobleaching. Fluorescence intensity at each site was determined as described in Materials and Methods. Error bars indicate SD (n = 3). The experiment was repeated three times with similar results.

Supplemental Figure 19

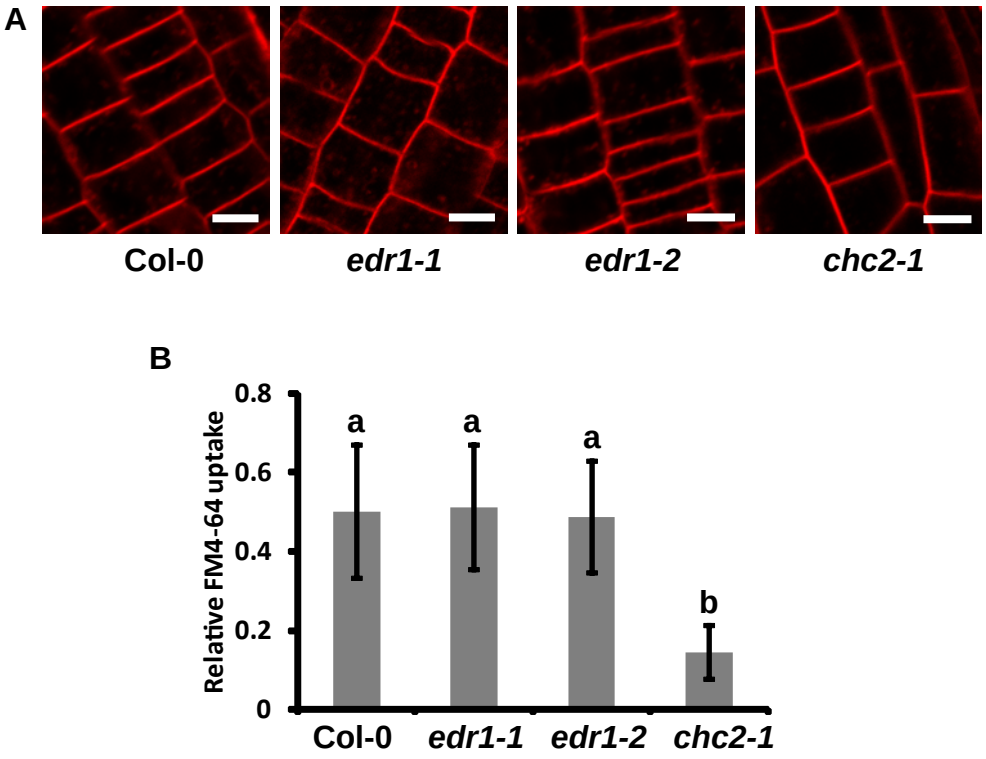

Supplemental Figure 19. The *edr1* mutant did not show defects in FM4-64 uptake.

(A) Intracellular accumulation of FM4-64 after incubation for 8 min in 2 μM FM4-64 in the root tip cells of five-day-old seedlings of wild type, *edr1-1*, *edr1-2*, and *chc2-1* mutants. Bars=10 μm.

(B) Quantification of relative FM4-64 uptake. The bars represent mean and standard deviation (n>50, number of cells analyzed). Statistically significant differences among the samples are labeled with different letters (P<0.01, one-way ANOVA). The experiment was repeated three times with similar results.

Supplemental Figure 20

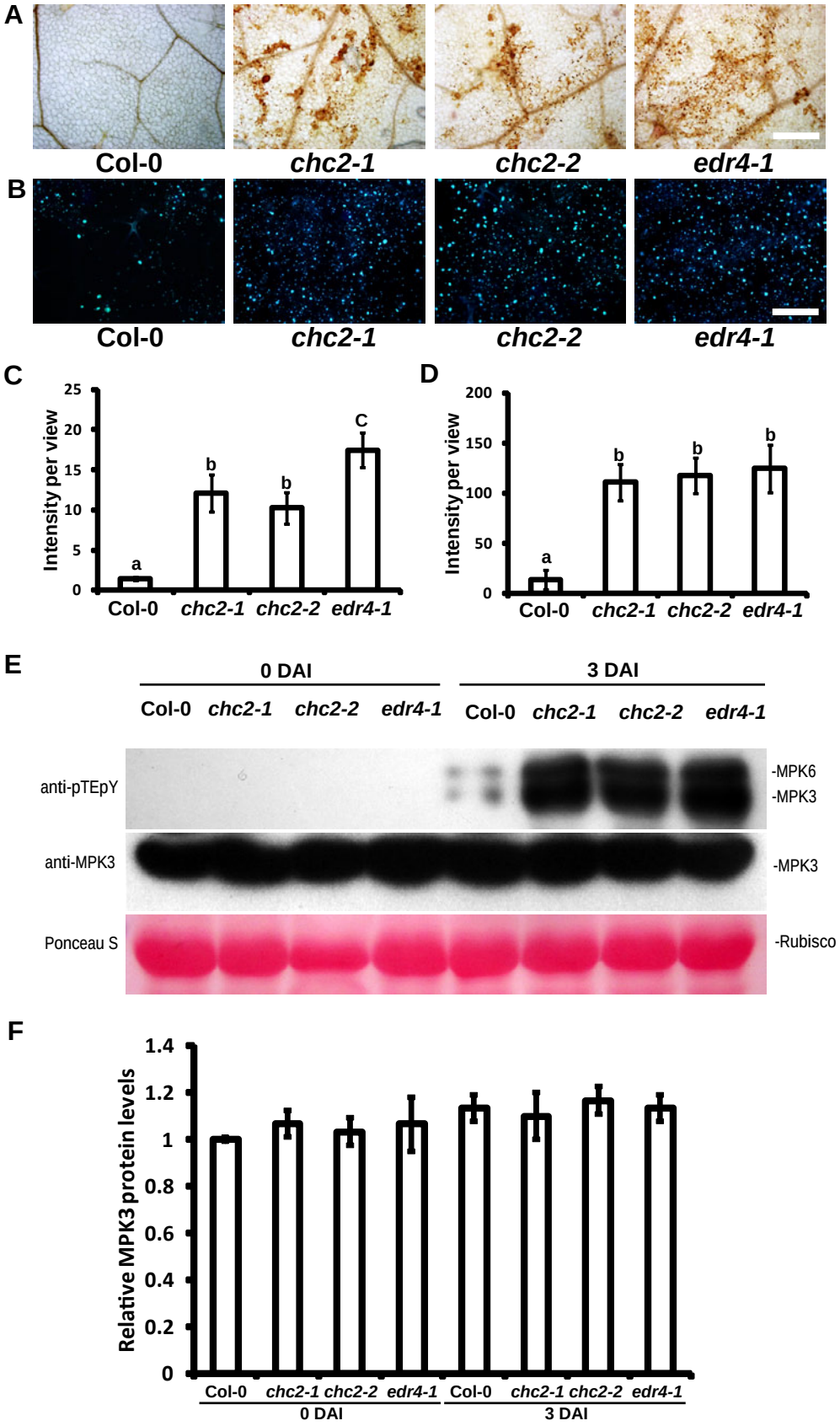

Supplemental Figure 20. The *chc2* mutants show increased accumulation of H_2O_2 and callose deposition and stronger MPK activation.

(A-B) DAB and Aniline blue staining of four-week-old wild type, *chc2-1*, *chc2-2*, and *edr4-1* plants at 2 dpi for H_2O_2 production and callose deposition, respectively. (A), DAB staining for H_2O_2 production; (B), Aniline blue staining for callose deposition; Bars=0.5 mm.

(C-D) Quantification of H_2O_2 production (C) and callose deposition (D) in plants from (A) and (B) respectively. The bars represent the mean and standard deviation of intensity per view from six leaves of three plants for each genotype. Statistically significant differences among the samples are labeled with different letters (P<0.01, one-way ANOVA). The experiment was repeated three times with similar results.

(E) MPK activation in four-week-old wild type, *edr4-1*, *chc2-1*, and *chc2-2* plants after powdery mildew infection, as shown by immunoblot analysis using anti-pTEpY antibody. The immunoblot assay with anti-MPK3 antibody shows MPK3 protein accumulation. Ponceau S staining of Rubisco is shown as a loading control.

(F) Relative MPK3 protein levels in (E) were calculated by ImageJ software with wild type at 0 DAI as the internal control. The bars represent mean and standard deviation (n=3).

Supplemental Table 1. Primers used in this study

Primers	Sequence	Notes
edr4-1-F	TCACAACAACCCAAGGGCAAGAGCT	dCAPS, SacI
edr4-1-R	ATCTCGGATGATACTCAGGTTG	
edr4-2-LP	CTGGTCTCCTCTCCCATTTTC	T-DNA
edr4-2-RP	AGCATTCCATTGTTCGTCATC	
edr4-3-LP	CGCAATGGGATTACCACATAC	T-DNA
edr4-3-RP	ATCAAGCCAAGAACGATGATG	
chc2-1-LP	CTCTAATTGGATCGCTGTTCG	T-DNA
chc2-1-RP	TGATTTCAACTTTGCTTTGGC	
chc2-2-LP	GTTCATGTTCGCCTGATTGTG	T-DNA
chc2-2-RP	CCTGATCTTACTGAGCACAAA	
pad4-1-F	CTGAGTTAGCCAATGAGCTTGCTAG	CAPS, KpnI
pad4-1-R	TCCACCATTTTAATCACTGGGTAC	
eds1-2-F	AGATCAATGGCGTTTGAAGCTCTTA	SSLP
eds1-2-R	ACCCCATCATGAGACCATTTCAATC	
mkk4-18-F	GGTTTAGCTTATCTCCATAGCCG	CAPS, HinfI
mkk4-18-R	CCTAAGCTCCAAATATCTCCAGC	
mkk5-18-F	GCCGCTAAAAGCTTATCCGCACTAGAA	CAPS, MseI
mkk5-18-R	GGGATGATCAACACTTCTTAAGATCTCGAGCT	
coi1-F	GGTTCTCTTTAGTCTTTAC	CAPS, XcmI
coi1-R	CAGACAACTATTTCGTTAC	
eds5-1-F	ATCTGATTCTTGATATGTTTGCCG	CAPS, HpaII
eds5-1-R	CGCCTGGTGAACAAGAAACAAC	
ein2-1-F	TTGCCAGAGAACATTCTAATGA	CAPS, AflII
ein2-1-R	GTTCCTTTACATCAGAGTCTTC	
edr1-F	AGGCTGAAAGGACAGATTCTTCATG	CAPS, HaeIII
edr1-R	TGTTGAGGAATTGTTCTCCAACTGA	
edr2-F	AGACAAGAACCATCATTATAGTGCTA	CAPS, BsmAI
edr2-R	AACAACACAACTTCACAGAAAGAGCA	
keg-4-F	ATGTGCAGCATGTCAAGAGC	CAPS, HaeIII
keg-4-R	CTTCATCTAAGCTGTGCATAAGGC	
sid2-2-F	AAACTGTTGCAGTCCGAAAGAC	SSLP
sid2-2-R	ATCTTCCTTCGTAAGTCTCCCT	
mpk3-1-LP	ATTTTTGTCAACAATGGCCTG	T-DNA
mpk3-1-RP	TCTGCCTTTTCACGGAATATG	
mpk4-LP	TTGCTCTGAATACACAGCAGC	T-DNA
mpk4-RP	GTCTTAGAGATCAGCGGGGAC	
mpk6-3-LP	CTCTGGCTCATCGCTTATGTC	T-DNA
mpk6-3-RP	ATCTATGTTGGCGTTTGCAAC	
npr1-63-LP	ATTTGTTTGAAGCACACCTGC	T-DNA
npr1-63-RP	CTCTCAAAGGCCGACTATGTG	
edr1-2-F	GTATCTCAAGGCATCGTGCTC	T-DNA

edr1-2-R	GTTTCCATAACGAGGATCACG	
RT-*ACT2*-F	AGTGTCTGGATCGGTGGTTC	Real time PCR
RT-*ACT2*-R	CCCCAGCTTTTTAAGCCTTT	
RT-*PR1*-F	GTGGGTTAGCGAGAAGGCTA	Real time PCR
RT-*PR1*-R	ACTTTGGCACATCCGAGTCT	
RT-*PR2*-F	TCGATGAGAATAAGAAGGAACCAAC	Real time PCR
RT-*PR2*-R	ATAACAACATACTACACGCTGAAAG	
RT-*PR5*-F	GCACAGAGACACACACAAAA	Real time PCR
RT-*PR5*-R	TGTTCCTTAGAGTGAAGTCTG	
EDR4 Complement-F	GCTCTAGAGGACTTGAGATAGCCCTACAAAACTT	for pCAMBIA1300
EDR4 Complement-R	GCGTCGACGTGCCTACTTACCTCTGACTCATCTA	
EDR4-GFP-F	CCCGTTAGTCATTGGATTGTGC	for pMDC107
EDR4-GFP-R	TATAGAAGGAGGACGCTGTGAAAC	
EDR4 Promoter-F	GCGAGCTCGACTTGAGATAGCCCTACAAAACTT	for pCAMBIA1300
EDR4 Promoter-R	GCTCTAGATGTTGGTACCAAATTTCAAAGACTT	
△CC-EDR4-CDS-F	GCTCTAGAATGATGAACACCGTAGCAGAAGC	for pCAMBIA1300
△CC-EDR4-CDS-R	GCGTCGACTATAGAAGGAGGACGCTGTGAAAC	
BiFC-N-CHC2-F	GCGTCGACGATGGCGGCTGCCAACGCCCCCATCA	BiFC
BiFC-N-CHC2-R	GGACTAGTTAATTAAGTAGCCGCCCATCGGTGGCATTCC	
BiFC-EDR4-F	GCGTCGACGATGGCGAGCCAGACGGGTC	BiFC
BiFC-EDR4-R	GGACTAGTTAATTAATATAGAAGGAGGACGCTGTGAAA	
BiFC-CC-EDR4-F	GCGTCGACGATGGCGAGCCAGACGGGTC	BiFC
BiFC-CC-EDR4-R	GGACTAGTTAATTAAATGAGACTCCAATCTGGAGTTG	
BiFC-LCR-EDR4-F	GCGTCGACGATGATGAACACCGTAGCAGAAG	BiFC
BiFC-LCR-EDR4-R	GGACTAGTTAATTAAGACATGACGCTTGGCCACA	
BiFC-DUF-EDR4-F	GCGTCGACGCGTCCAACAGCTGGTGG	BiFC
BiFC-DUF-EDR4-R	GGACTAGTTAATTAACTATATAGAAGGAGGACGCTG	
BiFC-KEG-F	GCGTCGACGATGGTTGGGAGAGTCAAGGT	BiFC
BiFC-KEG-R	GGACTAGTTAATTAAGCCAGAAGTTTCATCTAGAAC	
EDR4-T7-F	CCCCCGGGGATGGCGAGCCAGACGGGTC	Y2H
EDR4-T7-R	CGCGGATCCCTATATAGAAGGAGGACGCTGTGAAA	
△CC-EDR4-AD-F	CCCCCGGGGATGATGAACACCGTAGCAGAAG	Y2H
△CC-EDR4-AD-R	CGCGGATCCCTATATAGAAGGAGGACGCTGT	
CC-EDR4-AD-F	TTCATATGATGGCGAGCCAGACGGGTC	Y2H
CC-EDR4-AD-R	CGGAATTCATGAGACTCCAATCTGGAGTTG	
LCR-EDR4-AD-F	TTCATATGATGATGAACACCGTAGCAGAAG	Y2H
LCR-EDR4-AD-R	CGGAATTCGACATGACGCTTGGCCACA	
DUF-EDR4-AD-F	TTCATATGCGTCCAACAGCTGGTGG	Y2H
DUF-EDR4-AD-R	CGGAATTCCTATATAGAAGGAGGACGCTG	
KEG-AD-F	CCCCCGGGGATGGTTGGGAGAGTCAAGGT	Y2H
KEG-AD-R	CCATCGATGCCAGAAGTTTCATCTAGAAC	